Available online at www.sciencedirect.com

ScienceDirect

Procedia Structural Integrity 8 (2018) 14–23

Structural Integrity Procedia

www.elsevier.com/locate/procedia

AIAS 2017 International Conference on Stress Analysis, AIAS 2017, 6-9 September 2017, Pisa, Italy

Austempered Ductile Iron (ADI) for gears: Contact and bending fatigue behavior

Franco Concli[a]*

[a]*Free University of Bolzano/Bozen, piazza Università 1, Bolzano 39100, Italy*

Abstract

Austempered Ductile Iron (ADI) represents an alternative solution for the manufacturing of the housing of small planetary gearboxes, with the gear teeth obtained directly on the housing itself: such solution combines a cost-effective process with the possibility of obtaining complex geometry of the case. With respect to most traditional solutions, by means of ADI the requirements of strength and accuracy of the gear teeth can be satisfied without an additional finishing step after the heat treatment: the teeth can be obtained by broaching and, thanks to the low distortion which can be granted by the austempering process, a subsequent finishing operation is not needed. For these reasons, ADI has been selected for the application to a family of small gearboxes for automation. Due to the limited experience and data available for such material, to improve the design and rating processes, a testing campaign has been performed. The aim was to obtain strength data for bending and contact fatigue, considering the specific manufacturing and heat treatment processes. The paper describes the test procedures adopted and the test results, which have been obtained on gears specimens by means of Single Tooth Fatigue (STF) and pitting tests on a FZG type bench respectively. The tests are supported by metallurgical investigations on the failed teeth, to describe and understand the failure mechanisms. The results are then compared with the data and the shape curves provided by the international standards.

Peer-review under responsibility of the Scientific Committee of AIAS 2017 International Conference on Stress Analysis

Keywords: Austempered ductile iron; gears; bending; pitting; fatigue; tests

* Corresponding author. Tel.: +39-0471-017748; fax: +39-0471-017009.
E-mail address: franco.concli@unibz.it

Peer-review under responsibility of the Scientific Committee of AIAS 2017 International Conference on Stress Analysis
10.1016/j.prostr.2017.12.003

1. Introduction

Industrial planetary gearboxes used for automation require high torsional stiffness, low backlash and low tolerances to fulfil the requirements in terms of positioning accuracy (Concli (2016)). The housing is often manufactured in nodular cast iron, and the teeth of the ring gear manufactured in the casing by broaching. This ensures a cost-effective production process also for complex geometries of the casing. To meet the requirements of strength for the gear teeth a heat treatment is often required. To remove the distortions induced by the heat treatment, finishing operations are desired.

With the adoption of Austempered Ductile Iron (ADI), the requirements of strength and accuracy can be met without the final finishing operation: the teeth are manufactured by broaching and, thanks to the low distortion which can be granted by the austempering process, the subsequent finishing process is avoided.

The limited experience and available data for such class of materials have represented the main limitations to the large diffusion of ADI in the production of gears even if some applications can be found starting from the '80 (Vennemann et al. (1968), Ford (1968)).

A reliable estimation of the performances of a new material in terms of tooth root bending and contact fatigue resistance, can be obtained only performing tests on gear specimens. The use of data derived by standard specimens adapted to the gear rating would introduce a lot of uncertainties and hypotheses in the calculation method, with the unavoidable consequence that the performances rated would be only a rough estimation of the reality.

The Standard ISO 17804 (2005) provides bending and contact fatigue limits for ausferritic spheroidal graphite cast irons of different grades which could be used for design in combination with the curves for the life factors Y_{NT} and Z_{NT} (which practically define the shape of the S-N curve) to calculate the fatigue strength at different numbers of cycles (ISO 6336-5 (2003)), respectively for bending and pitting. Nevertheless, the ISO standards does not refer in an explicit way to ADI and the curves for different families of cast irons should be considered. The Information Sheet AGMA 939 (2005) provides bending fatigue and pitting limits, together with Y_N and Z_N factors specifically for ADI.

The analysis of the available data points out that the different existing standards provide:

- Different values of the limits and different dependency from the specific variant of the material and/or from other properties or other post treatment
- Different trends for the shape of the S-N curves
- Some shaded areas of scattering both for the values and for the trend of the S-N curves, and different assumptions concerning the region of the fatigue limit and the existence of the fatigue limit itself.

Based on the previous experiences of the author, which has performed and published several tests on gears materials (Gorla et al. (2017)), it can be stated that the fatigue strength of gears is influenced by many parameters that, combined, can determine large variations of the effective performances. In the context of the design of an innovative family of low backlash precision planetary gearboxes (Concli et al. (2017), Wehrle et al. (2017)) the performances of which must be granted accurately, a research program aimed at the experimental investigation of gear data has been conducted.

The test campaign has been performed on gear specimens representative of all the geometrical and technological properties of the real product, including the casting process, the tooth root geometry, the heat treatment, cutting and finishing processes and residual stresses.

The bending fatigue tests were performed with the STF (Single Tooth Fatigue) test method as shown in Gorla et al. (2012), while the pitting tests, for which the effective meshing condition must necessarily be reproduced, have been performed by means of an FZG type back-to-back test rig as shown by Gorla et al. (2014).

2. Material

The material is an ausferritic spheroidal graphite cast successively austempered. The chemical composition is reported in Tab. 1 while Tab. 2 shows the mechanical properties.

Table 1. Chemical composition of the base material.

C	Si	Cu	Ni	Mo	Mn
3.65	2.40	0.65	0.07	0.15	0.20

Table 2. Mechanical properties of the material.

HBW	UTS [MPa]	σ_y [MPa]	A [%]
308.7	830	572	10.2

According to the measured values (Tab. 2), the material can be classified as an ADI grade ISO 17804/JS/800-10.

A metallographic examination on one tooth of an untested gear specimen showed that the ADI had an ausferritic matrix structure (Fig. 1) (Martins (2008)).

Fig. 1. Austempered ductile iron microstructure (optical micrograph 500x after polishing and 4% nital etching).

3. Test

3.1. Bending Fatigue Tests

A 36-teeth - module 5 mm spur gear has been specifically designed. The main data of this gear are listed in Tab. 3.

Table 3. STF gear main data.

Description	Symbol	Value
Normal module	m_n	5 mm
Normal pressure angle	α_n	28 °
Tool tip radius coefficient	ρ^*_{fP}	0.375
Tool addendum coefficient	h^*_{fP}	1.296
Tool dedendum coefficient	h^*_{aP}	1.096
Shift coefficient	x	+0.200
Teeth number	z	36

The gear is mounted in a 65kN Schenck resonant fatigue testing machine as schematically shown in Fig 2. The gear is first mounted using a pin to fix its center; then a small pre-load is applied, in order to ”clamp” the two teeth being tested between the two anvils. The pin is removed, and, the test started. During the test, a sinusoidal load is applied at about 35 Hz. Even if the load of real gear teeth is pulsating from zero, the tests have been performed with a fatigue ratio R = 0.1, as usually done, since it is not possible to apply a zero load in this kind of tests. The aim of the bending test was to determine the fatigue limit through a staircase approach and, considering that typical ISO S-N curves assume that the knee is at $3 \cdot 10^6$ cycles, the run-out has been set at 5 million cycles. The staircase procedure has been defined according to Dixon (1965).

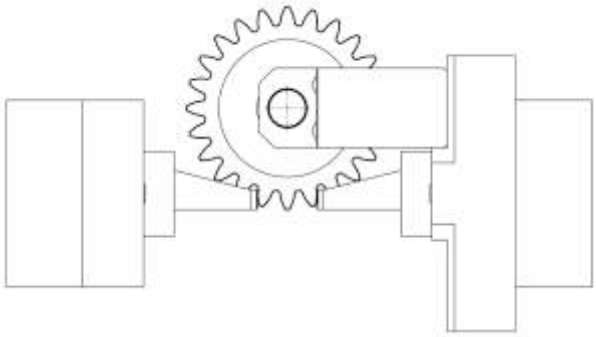

Fig. 2. Bending test schematic representation.

Fig. 3 summarizes the test results listed in Tab. 4, which includes also additional test points that are not considered in the staircase.

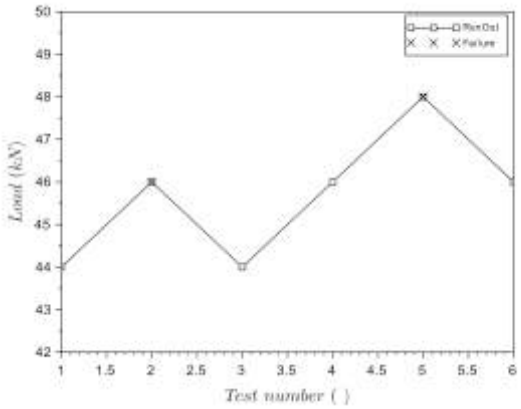

Fig. 3. Bending fatigue tests results.

Table. 4. Bending fatigue tests results.

Test ID	MAX Load [kN]	MIN Load [kN]	Cycles
Preliminary Tests (not used)			
0	-3.0	-30.0	RUNOUT
0	-3.4	-34.0	RUNOUT
0	-4.0	-40.0	RUNOUT
0	-4.2	-42.0	RUNOUT

Test ID	MAX Load [kN]	MIN Load [kN]	Cycles
Tests (used to define bending fatigue limit)			
1	-4.4	-44.0	RUNOUT
2	-4.6	-46.0	1611316
3	-4.4	-44.0	RUNOUT
4	-4.6	-46.0	RUNOUT
5	-4.8	-48.0	821414
6	-4.6	-46.0	RUNOUT

To obtain the fatigue limit (X_{50}) with 50% of probability of failure the following equation was used:

$$X_{50} = X_f + K \cdot d = 46 + 0.372 \cdot 2 = 46.7kN \tag{1}$$

where d is the load step and K is obtained by the table provided by Dixon (1965). The relations between the applied and measured forces and the tooth root stress have been calculated following the approach proposed by the ISO 6336-3 standard (2006).

$$Y_F = 6\frac{(h_F e / m_n)}{(s_F n / m_n)^2} \cdot \frac{cos\alpha_{Fen}}{cos\alpha_n} = 0.8678 \tag{2}$$

$$Y_s = (1.2 + 0.13 \cdot L) \cdot q_s^{\frac{1}{1.21+2.3/L}} = 2.5615 \tag{3}$$

$$\frac{\sigma_{F0}}{F} = \frac{Y_F \cdot Y_S}{b \cdot m_n} \cos \alpha_n \tag{4}$$

The stress value corresponding to a force of 1kN is equal to 10.44 MPa. The failure fatigue limit (50%) becomes

$$x_{50} = 487.55 MPa \tag{5}$$

The fracture surfaces of all the specimens were observed by means of a scanning electron microscope (SEM). It is worth pointing out that the fatigue behavior of the material under consideration, which is obtained by casting, can be influenced at a great extent by the defects, and by the porosity or cavities that could be typical spots of initiation. This consideration agrees with the fracture propagation mechanism in ADI described by Lin et al. (1996) based on an extensive experimental campaign on rotary bending fatigue. It must be also pointed out that, as explained and demonstrated by testing by Lin et al. (1996), who performed rotating bending fatigue tests on ADI specimens with different heat treatment parameters and different microstructures, the high cycle fatigue behavior of ADI can be significantly influenced by austempering temperatures and by the size and number of graphite nodules. For this reason, the knowledge of the microstructural properties of the tested specimen provides a necessary basis to check if the properties of components manufactured in the future are consistent with those of the specimens and therefore similar performances are reasonably to be expected. On the analyzed surfaces, the fracture does not seem to originate from a single point and beach marks have not been observed. It appears that the fractures originate from multiple local defects, like micro porosities or graphite nodules, especially if located next to the external surface. Fig. 4 shows examples of the surfaces of fracture. The SEM analyses have also confirmed that the maximum size of the micro-porosities was about 20μm, thus confirming that the casting process was producing specimens in accordance with the specifications.

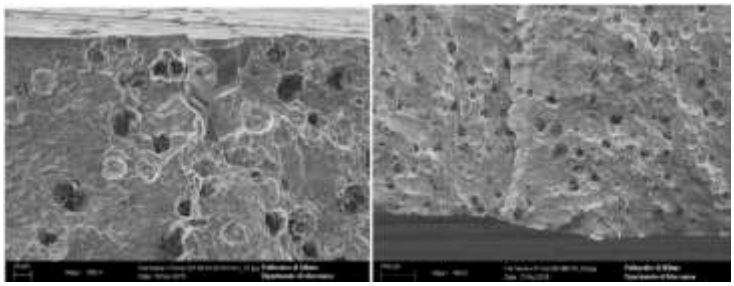

Fig. 4. Typical micro-porosity observed on tooth No. 14 of gear No. 1, failed after 821,414 cycles at 48 kN and nodules of graphite next to the external surface (tooth No. 7 of gear No. 4, failed after 1,611,316 cycles at 46 kN).

3.2. Surface Fatigue Tests

To investigate the surface fatigue strength, pitting tests were performed on a mechanical recirculating power test bench in the region between 10^6 and 10^7 cycles.

The test rig is a typical FZG type configuration made by a service- and a test-gearbox connected by two shafts in a closed mechanical power recirculation loop. The load can be introduced in the system (Fig. 5) acting on a rotating hydraulic controlled actuator mounted on one shaft.

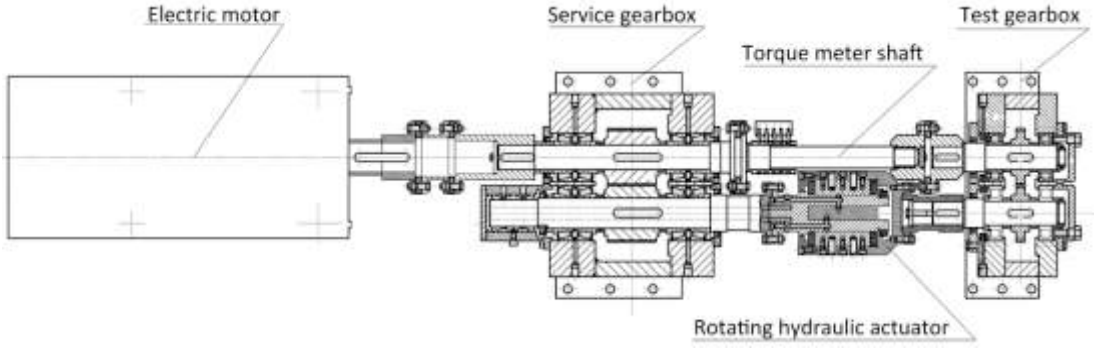

Fig. 5. Mechanical recirculating power test rig for tests on gears.

On the other shaft, a torque meter allows the measurement of the applied torque. The bench is actuated by an asynchronous motor, controlled by an inverter, which only needs to provide the power losses of the system. On the test bench two separate hydraulic circuits are present: one for the service gearbox and the hydraulic actuator and the other, the principal one, for the correct (and controlled) lubrication of the test gearbox.

The center distance is fixed and equal to 91.5 mm, the maximum applicable torque amounts at 1000 Nm and the maximum speed the electric motor can provide is 3000 rpm.

The main gear samples properties are reported in Tab. 5.

Table. 5. Surface fatigue gear sample properties.

Description	Sym.	Unit	Value	Description	Sym.	Unit	Value
Centre distance	a	mm	91.5	Tip diameter			
Face width	b	mm	14	Pinion	d_1	mm	99.509
Module	m	mm	5	Wheel	d_2	mm	104.206
Pressure angle	α	°	20	Tool b. rack profile			
Helix angle	β	°	0	Addendum per unit m	h^*_{aP0}	-	1.294
Number of teeth				Root fillet radius	ρ^*_{fP0}	-	0.375
Pinion	z_1	-	17	Flank Roughness	R_a	µm	0.94
Wheel	z_2	-	18	Accuracy grade	ISO AG 5		
Profile shift coef.				Heat treatment	Austempering		
Pinion	x_1	-	0.4753	Surface Hardness	309 HBW		
Wheel	x_2	-	0.4450	Profile modifications	None		

The gear pair was made of a pinion with 17 teeth and a gear with 18 teeth which, being prime numbers, determine the hunting teeth condition. The profile shift of the gears was selected to increase the bending strength with respects to the pitting resistance.

The three selected load levels are 200, 240 and 280 Nm. Each test was conducted at 3000 rpm. The gear samples were lubricated with an oil injection (ISO VG 220, with EP additives) at 60°C. All the tests were performed up to a pitting damage condition, except for a preliminary test at lower load which has been interrupted at 10^7 cycles. The failure condition, in accordance with the FVA-Information Sheet (1997), has been defined by convention as an extension of the damaged portion larger than 4% of the active surface on a single tooth flank. To detect the damage, the tests were regularly interrupted, with regular steps before the damage appearance and successively with closer steps to reach the limit condition.

Table. 6. Contact stresses and influencing factors at different test loads.

Description	Sym.	Unit	Value		
Pinion Torque	T_1	Nm	220	240	280
Contact stress					
Pinion	σ_{H1}	MPa	1049	1142	1228
Wheel	σ_{H2}	MPa	1039	1131	1216
Pitch contact stress	σ_{H0}	MPa	958	1050	1134
Zone Factor	Z_H	-	2.154		
Elasticity Factor	Z_E	-	170.833		
Contact ratio Factor	Z_ϵ	-	0.939		
Helix angle Factor	Z_β	-	1.000		
Single pair pinion	Z_B	-	1.034		
Single pair wheel	Z_D	-	1.024		
Application Factor	K_A	-	1.000		
Dynamic Factor	K_V	-	1.060	1.057	1.054
Face Load Factor	$H_{H\beta-C}$	-	1.056	1.047	1.040
Transversal Load Factor	$H_{H\alpha-C}$	-	1.000	1.000	1.000

Table 6 reports the calculated contact stresses.

The relations between the applied and measured torques and the contact stress have been calculated following the approach proposed by the ISO 6336-2 standard (2006).

$$\sigma_{H1/2} = Z_{B/D} \cdot \sigma_{H0} \cdot \sqrt{K_A \cdot K_V \cdot K_{H\beta} \cdot K_{H\alpha}} \tag{6}$$

$$\sigma_{H0} = Z_\epsilon \cdot Z_H \cdot Z_E \cdot \sqrt{\frac{F}{(d_1 \cdot b)} \frac{(u+1)}{u}} \tag{7}$$

Fig. 6 reports the SN curve for pitting.

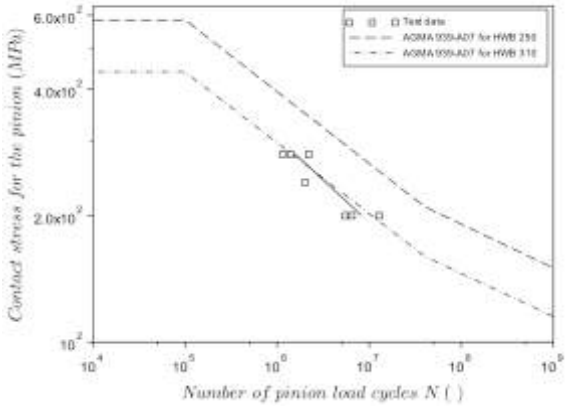

Fig. 6. Surface fatigue tests results

The method of linear least square proposed by ISO 12107 standard (2012) was used to fit the data. The trend of the S-N curve, in the range of fatigue lives considered, was assumed linear in a log-log diagram according to ISO 6336 (2006) and AGMA 939-A07 (2005). The diagram of Fig. 6, shows the σ_{HG}, "pitting stress limit" versus the number of cycles.

$$\sigma_{HG} = \sigma_{\lim} \cdot Z_L \cdot Z_V \cdot Z_R \tag{8}$$

The ISO standard does not provide the values of strength nor the factor Z_{NT} for ADI, so they were obtained by AGMA 939-A07 (2005). The results depicted in Fig. 6 were determined using the nominal hardness values. Even if the measurements of tooth flank hardness resulted in a higher average value (about 309 HBW), the test results were close to the minimum value of the range (corresponding to 250 HBW).

To monitor the evolution of the surface damage, the tests were interrupted each 0.5M cycles and visual inspections performed. In all the tests, the failure condition was reached because the limit extension of the damaged surface area was exceeded on one or few teeth of the pinion. While for high loads only the pinion flank was damaged, for the lowest load also the gear flanks show pitting. After the appearance of the first small pits on the surface of pinion teeth the failure occurs within less than 0.5M cycles. Both on pinion and gear teeth the damage occurs on the dedendum of the active flank, where the damage is promoted by a negative sliding condition. Fig. 7 shows an example of damage evolution.

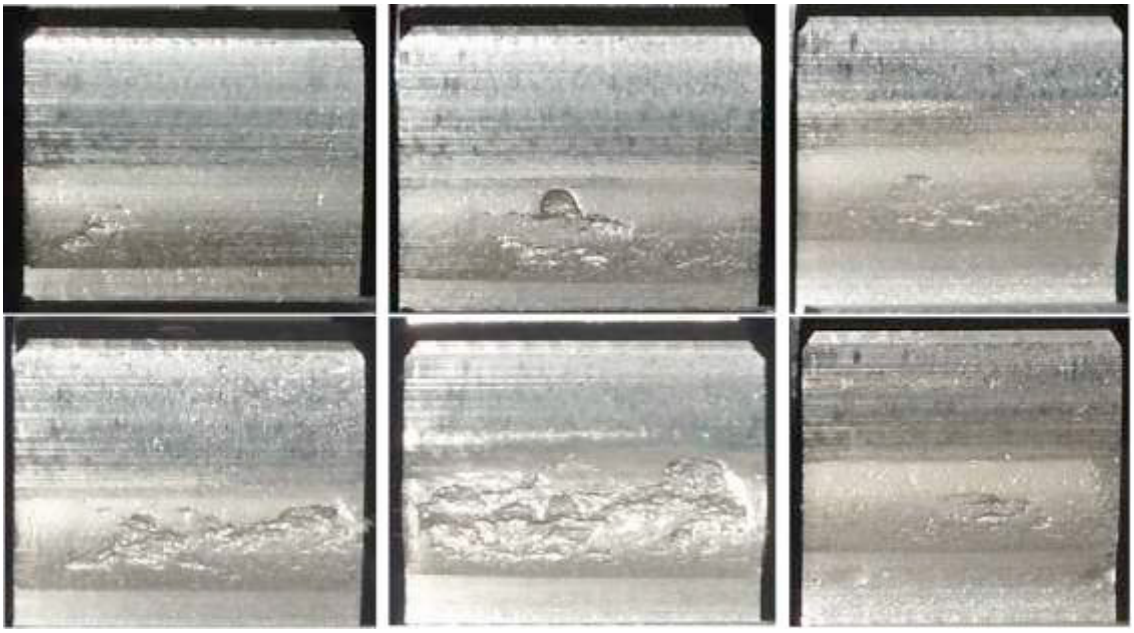

Fig. 7. Active flanks of three pinion teeth after: a) 2.0 million cycles at 280 Nm; b) 2.2 million cycles at 280 Nm (end of the test).

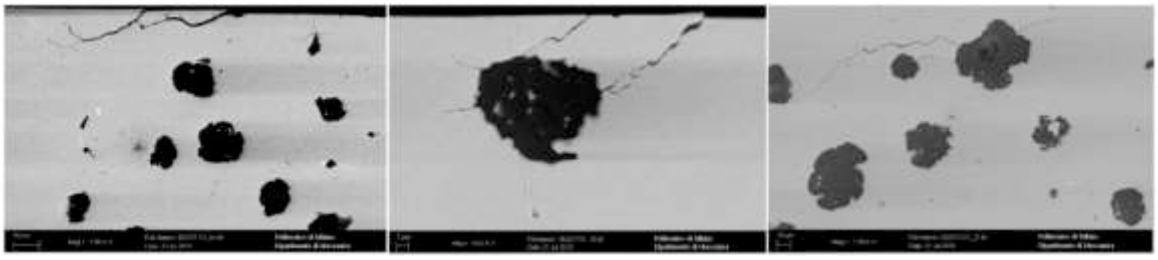

Fig. 8. Surface-breaking cracks propagating to form a micro-pit, interacting with a graphite nodule and propagating from and through graphite nodules and some surface cracks

SEM analysis were performed to better understand the failure mechanism. The surface breaking cracks were oriented at a shallow angle with respect to the contact surface (10 - 30°) and have, as typical in case carburized gears, opposite directions in the dedendum and the addendum of the tooth due to the presence of opposite sliding conditions. The formation of surface-breaking cracks in some cases seems to be related to the presence of graphite nodules close to the contact surface (Fig. 8), but in some others, does not: surface-breaking cracks located over and connected to a

graphite nodule were found, as previously observed by Magalhaes et al. (2000) in experiments with discs at a higher contact pressure level, but also surface-breaking fractures not interacting with graphite nodules were found.

The propagation path of cracks seems to be significantly influenced by the presence of graphite nodules both in the formation of micro-pits and in the developments of macro-pits or spalls.

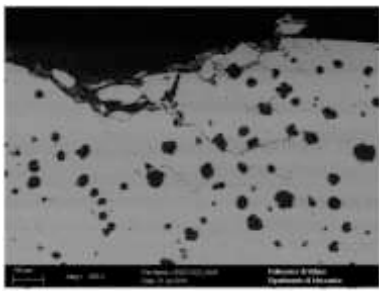

Fig. 9. Macro-pit with propagating branching cracks

Few subsurface cracks propagating from and through graphite nodules were found located in the range 20–100μm below the contact surface as shown for example in Fig. 8. The deepest of these cracks was close to the region where the maximum stress level due to Hertzian contact pressures can be located using multiaxial fatigue criteria (as proposed in Conrado et al. (2011) and Davoli et al. (2003)). Since macro-pits or spalls have a typical depth of about 100—200μm, the present analysis suggested that the macro-pits or spalls can be originated, in this type of material, by subsurface cracks that eventually interact with surface cracks or micro-pits and develop by means of the propagation of branching cracks interacting with graphite nodules as shown in Fig. 9.

4. Conclusions

The tooth root bending and surface contact fatigue limits for an Austempered Ductile Iron (ADI) to be used in gearbox rating procedures have been determined experimentally, by specifically designing and manufacturing specimens that could be representative of the effective status of the real product, including casting process, machining, heat treatment, local geometry, roughness, residual stresses, etc.. The tests have been performed with the STF (Single Tooth Fatigue) approach for bending and with a recirculating power test bench on meshing gears for pitting. The data obtained, after the necessary calculation to consider the load-stress relation and the statistical effects, have been compared with those provided by ISO Standard and AGMA Information Sheets. The comparison has shown that the results of the present research are in the ranges provided by these documents. The tests have therefore provided results that on one side are validated by the previous knowledge but that on the other side are more accurate for the specific application.

References

AGMA 939-A07 - Austempered Ductile Iron for Gears - AGMA Information Sheet, 2005.

Concli, F., 2016, Thermal and efficiency characterization of a low-backlash planetary gearbox: An integrated numerical-analytical prediction model and its experimental validation, Proceedings of the Institution of Mechanical Engineers, Part J: Journal of Engineering Tribology, 230 (8), pp. 996-1005.

Concli, F., Gorla, C., 2017, Numerical modeling of the churning power losses in planetary gearboxes: An innovative partitioning-based meshing methodology for the application of a computational effort reduction strategy to complex gearbox configurations, Lubrication Science, DOI: 10.1002/ls.1380.

Conrado, E., Foletti, S., Gorla, C., et al., 2011, Use of multiaxial fatigue criteria and shakedown theorems in thermoelastic rolling sliding contact problems. Wear 2011; 270: 344–354, DOI: 10.1016/j.wear.2010.11.004.

Davoli, P., Bernasconi A., Carnevali, L., 2003, Application of multiaxial criteria to contact fatigue assessment of spur gears, Proceedings of DETC'03, ASME 2003 Design Engineering Technical Conference and Computers and Information in Engineering Conference, Chicago, Illinois, USA, September 2–6.

Dixon, W., J., 1965, The Up-And-Down Method for Small Samples, American Statistical Association Journal, December 1965, pp. 967-978.
Ford, L., 1968, Lufkin's austempered gear testing program, 2nd International Conference on Austempered Ductile Iron: Your Means to Improved Performance, Productivity and Cost.; Ann Arbor, MI, USA; ; Code 9174
FVA-Information Sheet -Research Project No.2/IV - Pitting Test, 1997.
Gorla, C., Rosa, F., Concli, F., Albertini, H., 2012, Bending fatigue strength of innovative gear materials for wind turbines gearboxes: Effect of surface coatings, ASME 2012 International Mechanical Engineering Congress and Exposition, IMECE 2012; Houston, TX; United States; 9 November 2012 through 15 November 2012; Volume 7, Issue PARTS A, B, C, D, 2012, Pages 3141- 3147, DOI: 10.1115/IMECE2012-86513.
Gorla, C., Rosa, F., Conrado, E., Albertini, H., 2014, Bending and contact fatigue strength of innovative steels for large gears, Proceedings of the Institution of Mechanical Engineers, Part C: Journal of Mechanical Engineering Science, Volume 228, Issue 14, 27 October 2014, Pages 2469-2482, DOI: 10.1177/0954406213519614.
Gorla, C., Conrado, E., Rosa, F., Concli, F., 2017, Contact and bending fatigue behaviour of austempered ductile iron gears, Proceedings of the Institution of Mechanical Engineers, Part C: Journal of Mechanical Engineering Science, DOI: 10.1177/0954406217695846.
ISO 12107:2012(E) Metallic materials - Fatigue testing - Statistical planning and analysis of data, 2012.
ISO 17804:2005(E) Founding - Ausferritic spheroidal graphite cast irons – Classification, 2005.
ISO 6336-2:2006(E) Calculation of load capacity of spur and helical gears - Part 2: Calculation of surface durability (pitting), 2006.
ISO 6336-5:2003(E) Calculation of load capacity of spur and helical gears - Part 5: Strength and quality of materials, 2003.
Lin, C.-K., Lai, P.-K., Shih, T.-S., 1996, Influence of microstructure on the fatigue properties of austempered ductile irons - I. Highcycle fatigue. Int J Fatigue 1996; 18(5):297–307.
Magalhaes, L., Seabra, J., Sa, C., 2000, Experimental observations of contact fatigue crack mechanisms for austempered ductile iron (ADI) discs, Wear 246 (2000) 134-148, DOI: 10.1016/S0043-1648(00)00493-2.
Martins, R., Seabra, J., Magalhães, L., 2008, Austempered ductile iron (ADI) gears: Power loss, pitting and micropitting, Wear, 264 (9-10), pp. 838-849.
Moore, W., 1987, ADI in perspective, Cast World, 19 (1), pp. 16-23.
Vennemann, K., Hornung, K., Fischer, G., 1986, Gears made of adi for the automotive industry, 2nd International Conference on Austempered Ductile Iron: Your Means to Improved Performance, Productivity and Cost.; Ann Arbor, MI, USA; ; Code 9174, pp. 373-379
Wehrle, E. J., Concli, F., Cortese, L., Vidoni, R., 2017, Design optimization of planetary gear trains under dynamic constraints and parameter uncertainty, ECCOMAS Thematic Conference on Multibody Dynamics, June 19-22, 2017, Prague, Czech Republic